ELSEVIER

Biophysical Chemistry 125 (2007) 483–489

Biophysical Chemistry

http://www.elsevier.com/locate/biophyschem

Residue cluster additivity of thermodynamic stability in the hydrophobic core of mesophile vs. hyperthermophile rubredoxins

David M. LeMaster, Griselda Hernández*

Wadsworth Center, New York State Department of Health, and Department of Biomedical Sciences, University at Albany - SUNY, Empire State Plaza, Albany, New York 12201-0509, USA

Received 5 October 2006; received in revised form 27 October 2006; accepted 27 October 2006
Available online 22 November 2006

Abstract

The branched sidechain residues 24 and 33 in the hydrophobic core of rubredoxin differ between the *Clostridium pasteurianum* (*Cp*) and *Pyrococcus furiosus* (*Pf*) sequences. Their X-ray structures indicate that these two sidechains are in van der Waals contact with each other, while neither appears to significantly interact with the other nonconserved residues. The simultaneous interchange of residues 24 and 33 between the *Cp* and *Pf* rubredoxin sequences yield a complementary pair of hybrid proteins for which the sum of their thermodynamic stabilities equals that of the parental rubredoxins. The 1.2 kcal/mol change arising from this two residues interchange accounts for 21% of the differential thermodynamic stability between the mesophile and hyperthermophile proteins. The additional interchange of the sole nonconserved aromatic residue in the hydrophobic core yields a 0.78 kcal/mol deviation from thermodynamic additivity.

Keywords: Hydrophobic core; Proteins; Thermostability; Thermodynamic additivity; NMR chemical exchange; Chimeric hybrids

1. Introduction

Microbial life thrives at temperatures ranging from the freezing point to the boiling point of water. Likewise, the constituent proteins exhibit a wide range of thermal stabilities that generally reflect the growth conditions of the corresponding organism. Both practical and theoretical interest in how these differential stabilities have evolved stimulates the ongoing comparisons of structurally homologous proteins derived from organisms adapted to markedly different environments.

If the introduction of a residue from a thermophile protein into the sequence of a homologous mesophile protein yields an increase in thermodynamic stability, then this residue is generally considered to account for at least the corresponding proportion of the overall difference in stability between the parental mesophile and thermophile proteins. On the other hand, a quantitative estimate of the differential stability contribution can only be obtained if the introduction of the complementary sequence change into the thermophile sequence results in an equivalent decrease in thermodynamic stability. In the most straightforward case, each residue interchange provides an increment in stability that is independent of the other residues that are not conserved between the two homologous protein sequences. However, only for the cold shock protein [1,2] and cytochrome c_{551} [3,4] has it been directly demonstrated that a small subset of the residues differing between the mesophile and thermophile homologs, each providing an approximately independent increment in stability, fully account for the large (>20 °C) difference between the T_m values of the parental proteins.

When there are significant interactions between two or more nonconserved residues in a given parental structure such that equivalent interactions can not be formed upon exchange of each such residue into the other parental protein, then independent additivity of stability for the individual residues can not be expected to apply. In this circumstance, it may be asked whether the simultaneous interchange of a cluster of nonconserved residues could yield equal and opposite changes in the thermodynamic stability for the resultant complementary pair of hybrid proteins. This question is particularly germane to buried residues for which double mutant cycle analysis of

* Corresponding author. Tel.: +1 518 474 4673; fax: +1 518 473 2900.
E-mail address: griselda@wadsworth.org (G. Hernández).

0301-4622/$ - see front matter © 2006 Elsevier B.V. All rights reserved.
doi:10.1016/j.bpc.2006.10.013

interaction energies [5,6] can be limited by the assumption that the protein structure is unperturbed by the mutational exchange. We [7] recently reported an algorithm designed to identify clusters of nonconserved residues that can be interchanged between a pair of structurally homologous proteins so as to potentially maintain the parental-like interactions across the putative hybridization interface.

The rubredoxin from *Pyrococcus furiosus* (*Pf*) was the first hyperthermophile protein for which an X-ray [8] as well as an NMR [9] structure were reported. In its role as a model for this class of proteins, numerous hypotheses have been offered as to which aspects of the structure yield increased thermostability relative to the homologous rubredoxins from mesophilic organisms. As for many of the other proteins derived from hyperthermophilic organisms [10,11], rubredoxin does not reversibly unfold under typical thermal or denaturant conditions, thus precluding quantitative interpretation of the thermodynamic effects for systematic mutational analysis. However, recently we [12] found that the rapid reversible unfolding of the mesophile and thermophile rubredoxins can be monitored in the presence of the much slower irreversible denaturation process.

In applying the residue cluster analysis algorithm [7], we found that seven nonconserved residues of the metal binding site region could be interchanged between the sequences of *Pf* rubredoxin and the structurally homologous protein from *Clostridium pasteurianum* (*Cp*) to yield a pair of complementary hybrids with free energies of stability that differ symmetrically from the corresponding parental protein values by slightly over 2 kcal/mol. This $\Delta\Delta G$ value corresponds to 39% of the differential stability for the mesophile and hyperthermophile rubredoxins arising from these seven residues [13]. These rubredoxin chimeras appear to provide the first example of a complementary pair of hybrids systematically designed from known parental protein structures that exhibit full thermodynamic additivity upon exchange of a cluster of mutually interacting nonconserved residues that define a substantial hybridization interface (360 A^2) across the core of a protein domain.

In the present study, the residue cluster analysis was applied to further characterize the structural contributions to the differential stability of the rubredoxins. Of particular interest for thermostability analysis of rubredoxin is its hydrophobic core which is composed of five highly conserved aromatic residues, one less strongly conserved aromatic residue and several aliphatic residues. Recently, ab initio calculations [14,15] have been applied to the rubredoxin hydrophobic cluster to assess the energy stabilization arising from these interactions. Neutron and X-ray diffraction [16] as well as NMR studies on the metal-free state [17] have been carried out on a *Pf* rubredoxin containing *Cp*-derived residues at the nonconserved aromatic position and the two nonconserved branched sidechain amino acids at positions 24 and 33 within the core. With the same interaction criteria as were used to identify the seven residue cluster, the branched aliphatic sidechains at positions 24 and 33 were predicted to form a two residue nonconserved cluster. Stability measurements were conducted on the hybrids of *Cp* and *Pf* rubredoxins formed by interchange of residues 24 and 33, both singly and as a pair. In addition, the nonconserved aromatic core residue was also interchanged. ^{1}H NMR thermal chemical exchange measurements established the degree to which these pairs of complementary hybrids exhibit additivity in their thermodynamic stabilities relative to the parental proteins.

2. Materials and methods

2.1. Sample preparation

Escherichia coli codon-optimized genes for *Cp* and *Pf* A2K [18] rubredoxins in the plasmid pT7-7 [19] were altered at residues 4, 24, and 33 by site-directed mutagenesis (QuikChange, Stratagene). The mutagenesis reactions were performed for 18 cycles in Perkin-Elmer Gene Amp PCR System (Model 9600) according to the manufacturer's recommended procedure. Expression of the rubredoxin proteins was carried out in the BL21(DE3) system (Novagen), modified by introduction of a second plasmid, which constitutively overproduces the methionine peptide deformylase to yield homogenous N-terminal processing [18]. The protein samples were purified as previously described [20].

2.2. NMR measurements

The protein samples were concentrated and exchanged by centrifugal ultrafiltration into 100 mM sodium borate buffer in D_2O at a pD* of 9.08, where *p*D* is the uncorrected reading on a ^1H_2O saturated electrode. The protein solution was aliquoted into multiple NMR pressure tubes (No. 524-PV-7; Wilmad Glass, Buena, NJ), and O_2 was purged by repeated flushing with nitrogen. The tubes were then sealed under 35 psi of N_2 to help reduce reflux at higher temperatures. Spectrometer temperature calibration was carried out with 80% ethylene glycol in dimethylsulfoxide-d_6 (WGH-130; Bruker BioSpin Corp., Billerica, MA). Data collection and the temperature-dependent chemical shifts corrections were conducted as previously described [12]. The chemical shifts for resonances shifted more than 1 ppm in the native state were normalized to the difference between the native state and model peptide values [21] to yield population estimates for the folded and reversibly unfolded states. These values were fitted to the Gibbs–Helmholtz equation:

$$\Delta G^o(T) = \Delta H^o(T_m)(1-T/T_m) - \Delta C_p^o[(T_m - T) + T\ln(T/T_m)]$$

with ΔC_p set to 0.5 kcal mol^{-1}, typical for a protein of this size [22]. The data from each resonance were weighted by the magnitude of the nonlinear temperature-dependent change in frequency monitored by that resonance.

3. Results and discussion

3.1. Exchange of residues 24 and 33 in Cp rubredoxin

In the X-ray structure of *Cp* rubredoxin [23], the C^δ of Ile 33 is surrounded by the aromatic sidechains of Tyr 13, Phe 30,

and Trp 37 as well as by the sidechain methyls of Val 24 and Thr 28 (Fig. 1). The ring current effects from these aromatic residues cause the Ile 33 H^{δ} resonance to be shifted by more than 2 ppm upfield. Substitution of leucine at this position results in a further 0.5 ppm upfield shift for the $H^{\delta 1}$ under similar conditions, approximately equal to the shift observed for this leucine methyl resonance in *Pf* rubredoxin. With the exception of Val 24, all of the residues containing atoms within 6 Å of Ile 33 C^{δ} are conserved in sequence and conformation in *Pf* rubredoxin [24].

Although the rubredoxins exhibit irreversible denaturation behavior under typical calorimetric conditions, we have observed that the wild type *Cp* and *Pf* [12] and various hybrid [13,25] rubredoxins undergo a reversible unfolding transition which can be directly monitored via the chemical shift migration of the strongly shifted resonances as a function of temperature. Both *Cp* and *Pf* rubredoxins (un)fold in approximately 40 μs at their thermal transition temperatures so that the chemical exchange effect results in ^{1}H resonances that are a weighted average of the chemical shifts for the folded and reversibly unfolded species, as illustrated in Fig. 2 for the upfield shifted methyl resonances of the I33L variant of *Cp* rubredoxin.

^{1}H NMR thermal chemical exchange measurements have been carried out on a number of proteins that reversibly unfold in the μs-ms timeframe [26–31]. The varying linewidth and migrating chemical shifts of the monitored resonances report the rate of the reversible unfolding transition and the populations of the folded and unfolded states, respectively. Only the reversibly refolding species contribute to these dynamically averaged resonances. The accumulation of irreversibly denatured protein that occurs during data acquisition on the rubredoxins increases the signal intensity for resonances near the random coil shift values and reduces the fraction of protein undergoing the reversible unfolding transition. However, the irreversibly denatured component only indirectly affects the monitored resonances of the reversibly refolding species via the resultant decrease in their intensity.

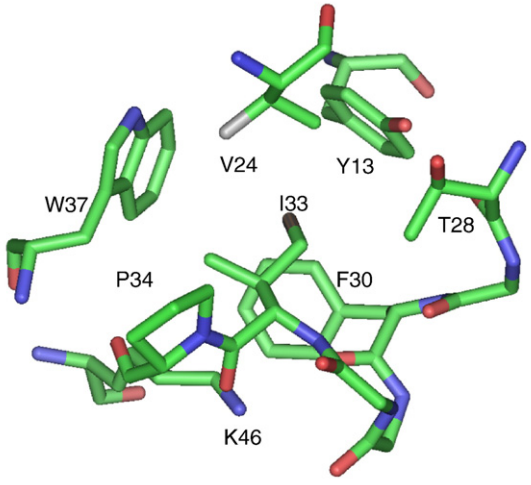

Fig. 1. The hydrophobic core of *Cp* rubredoxin surrounding the sidechain of Ile 33. The C^{δ} of Ile 33 is colored in black. The $C^{\gamma 2}$ position of Val 24, which is transformed into an ethyl group upon substitution of isoleucine, is colored in white. All residues containing atoms within 6 Å of the Ile 33 C^{δ} atom are shown.

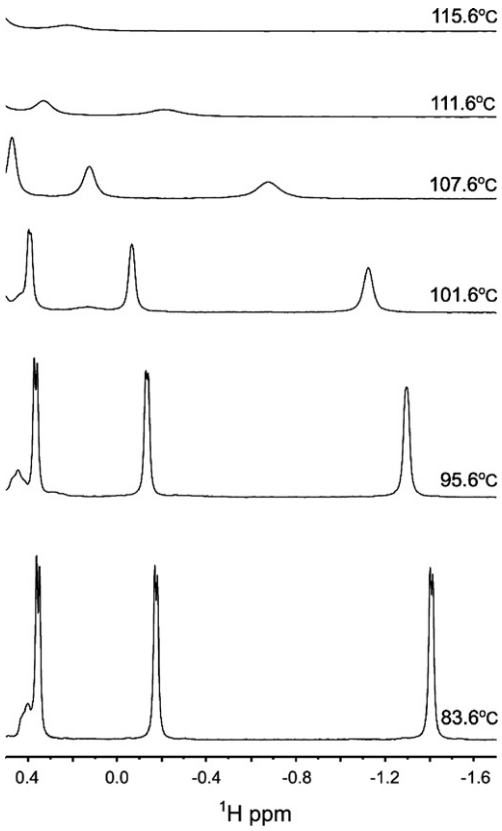

Fig. 2. Chemical exchange dynamics in the ^{1}H NMR spectrum of the I33L variant of *Cp* rubredoxin. Illustrated is the upfield methyl spectral region as a function of temperature. Leu 33 $H^{\delta 1}$ and Leu 33 $H^{\delta 2}$ are the two most strongly upfield shifted resonances. The amplitude of the signals decreases at higher temperatures, due to both the dynamic broadening of the resonances and the loss of signal intensity into the irreversibly denatured protein component.

In general, protein thermal chemical exchange studies have focused on the resonance broadening effect to measure the rate of interchange between the folded and unfolded states as a function of temperature. Due to the favorable characteristics of the rubredoxins, these experiments also provide accurate determinations of the folding equilibria up to near 144 °C, the T_m of wild type *Pf* rubredoxin [12], a value 40° above the highest reversible T_m for a monomeric protein reported by calorimetric methods [32]. In addition to the Leu 33 methyl resonances illustrated in Fig. 2 (and the analogous Ile 33 C^{δ} resonance of the parental *Cp* rubredoxin), the resonances of the conserved core residues Phe 30 H^{δ}, Trp 37 $H^{\zeta 3}$, and Phe 49 H^{α} are generally well resolved in the native state and are all shifted by at least 1 ppm from their random coil values. The temperature-dependent migrations for each of these resonances provide independent monitors of the unfolding transition.

Since in most cases the peak shifts are easily measured to within a Hz, the population of reversibly unfolded species at levels of 1% or less can be accurately determined, depending only on the reliability of the estimated reference shifts for the native and reversibly denatured states. The broad thermal stability range of the rubredoxins enables demonstration of the

linear temperature dependence for the native state chemical shifts of these strongly shifted resonances, which can then be used to extrapolate the native state resonance frequency into the thermal transition [12,13,25]. Since the chemical shifts for the reversibly unfolded state can not be directly observed for the rubredoxins, reference peptide values [21] are assumed. The precise consistency of each of these strongly shifted ^{1}H resonances with the thermal dependence of the Gibbs–Helmholtz equation [12,13,25] is consistent with a two-state transition. Furthermore, the consistency among the population estimates for various resonances vindicate the use of model peptide referencing for the reversibly unfolded state, since deviations in those reference values of more than 0.1–0.2 ppm can be detected by the divergence of the corresponding curve [12].

In Fig. 3A are given the unfolded state population values as a function of temperature, derived from the upfield methyl resonance of residue 33 in wild type *Cp* rubredoxin (●) as well as the V24I (▲) and I33L (▼) single mutants, the V24I, I33L (■) double mutant and the Y4W, V24I, I33L (★) triple mutant of the parental *Cp* protein. The accompanying curves represent the optimal fits of the Gibbs–Helmholtz equation to the combined chemical shift migration patterns of the Phe 30 H^{δ}, Trp 37 $H^{\zeta 3}$, Phe 49 H^{α} and Leu (or Ile) 33 H^{δ} methyl resonances. Introduction of the residues 24 and 33 from the hyperthermophile sequence into *Cp* rubredoxin, either singly or as a pair, yields an increase in thermal stability.

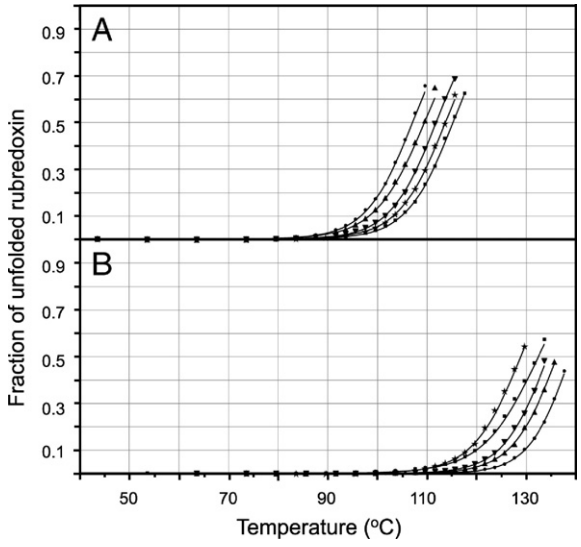

Fig. 3. Reversible unfolding equilibria for wild type and hydrophobic core variants of rubredoxin. The symbols in panel A indicate the fraction of reversibly unfolded species as a function of temperature, as monitored by the chemical exchange analysis, for wild type *Cp* rubredoxin (●), the V24I (▲) and I33L (▼) single mutants, the V24I, I33L (■) double mutant, and the Y4W, V24I, I33L (★) triple mutant of the parental *Cp* protein, as determined from the most strongly upfield shifted methyl resonance (i.e., Leu 33 $H^{\delta 1}$ or Ile 33 H^{δ}). Optimal fits to the modified Gibbs–Helmholtz equation were obtained from combined chemical shift migration patterns of the Phe 30 H^{δ}, Trp 37 $H^{\zeta 3}$, Phe 49 H^{α} and Leu (or Ile) 33 H^{δ} methyl resonances. In panel B, the analogous population data for the parental hyperthermophile *Pf* A2K (●), the single-residue variants I24V (▲) and L33I (▼), the double-residue variant I24V, L33I (■), and the W4Y, I24V, L33I (★) triple mutant. The spectra collected more than 30° below the T_m values were used to determine a linear temperature dependence of the relative native state chemical shifts. The fraction of unfolded protein is derived from the observed chemical shift normalized to the difference between the native state and model peptide chemical shifts [21].

These thermal chemical exchange measurements allow the fraction of reversibly unfolded species, and hence the free energy of stability, to be directly determined under the same temperature conditions for a series of related proteins. As a result, one can avoid the model-dependent extrapolations standardly invoked when $\Delta\Delta G$ values are estimated for such a set of proteins. At 107.6 °C, the $\Delta\Delta G$ for unfolding of the wild type, the V24I and I33L single-residue variants, and the V24I, I33L variant of *Cp* rubredoxin are 0.36, 0.76, and 1.31 kcal/mol, respectively. The independent population estimates derived from the individual monitored resonances yield an estimated uncertainty of 0.09 kcal/mol in the $\Delta\Delta G$ values for these three variant rubredoxins, relative to the wild type *Cp* protein.

3.2. Comparison of interchanging residues 24 and 33 in *Pf* vs. *Cp* rubredoxin

Thermal chemical exchange experiments were also carried out on the hyperthermophile rubredoxin (●) and the single-residue variants I24V (▲) and L33I (▼), as well as the double-residue variant I24V, L33I (■) (Fig. 3B). The pattern of decreasing thermal stability arising from these substitutions of residues from the mesophile *Cp* rubredoxin sequence closely mirrors the pattern of increasing stabilization for the complementary substitutions into *Cp* rubredoxin (Fig. 3A). For these studies, an A2K variant of *Pf* rubredoxin [18] has been utilized as the parental reference, since this protein retains the N-terminal methionine and exhibits interactions at that terminus which mimic those of *Cp* rubredoxin. The T_m value for *Pf* A2K rubredoxin is 7 °C below that of the wild type *Pf* protein [12]. The free energies of stability for the complementary *Pf* A2K rubredoxin variants were analyzed at 133.6 °C. The differential free energies of each variant, relative to the parental proteins, are illustrated in Fig. 4.

Introduction of residues from *Pf* rubredoxin into the *Cp* protein sequence at positions 24 and 33 gives rise to increases in thermodynamic stability of 0.36 and 0.76 kcal/mol, respectively (Fig. 4A), while the complementary mutations in *Pf* A2K rubredoxin yielded decreases in thermodynamic stability of 0.55 and 0.88 kcal/mol, respectively (Fig. 4B). The magnitudes of the $\Delta\Delta G$ values are similar to those recently reported for an analogous reciprocal interchange of Val and Ile at position 30 of the homologous hyperthermophilic Sac7d and Sso7d proteins [33]. However, the sum of the increments in stability for the two single mutants of the rubredoxins is somewhat less than the stability increase resulting from the combined V24I, I33L mutations, suggesting a modest degree of synergy between the two sites. Similarly, the sum of the decreases in stability arising from the complementary single mutations in the *Pf* A2K background appreciably exceeds the destabilization arising from the combined I24V, L33I mutations (Fig. 4B).

As the population estimates within panel A and within panel B of Fig. 4 are obtained under the same experimental conditions, to the accuracy of these populations, the $\Delta\Delta G$ values are independent of any assumption regarding a two-state transition

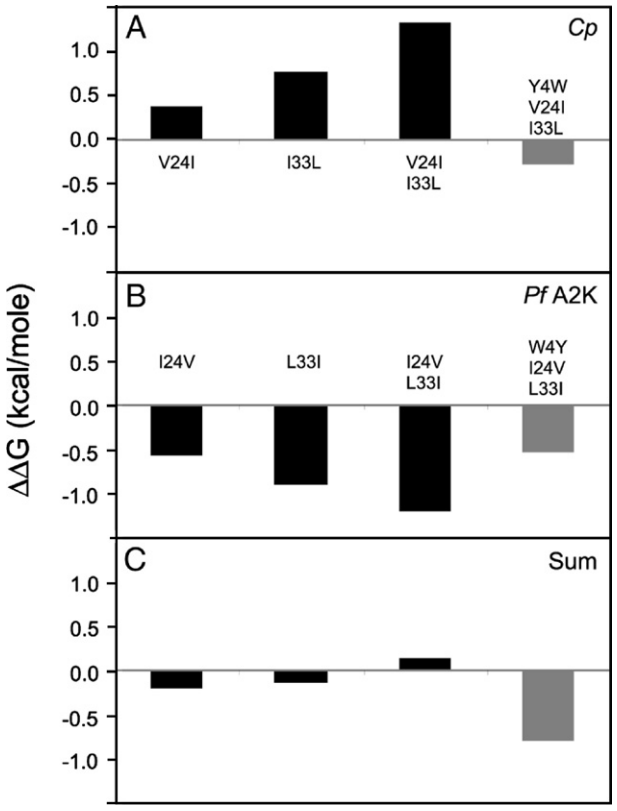

Fig. 4. Differential free energies of stability for the hydrophobic core variants as compared to those of the parental mesophile and hyperthermophile rubredoxins. The $\Delta\Delta G$ values for the variants at residues 24 and 33 are given with respect to *Cp* rubredoxin (panel A) and *Pf* A2K rubredoxin (panel B). Panel C illustrates the net additivity of the sum of the thermodynamic stabilities of the complementary pairs of hybrids as compared to those of the two parental rubredoxins. Given the additivity in thermodynamic stability observed for the residues 24 and 33 double mutation, the differential free energies for the additional mutation at residue 4 (gray) are referenced to those of the double mutant.

or heat capacity value. However, as the temperature differs between the data of panel A and that of panel B, direct comparison between these two data sets requires the additional assumption that $\Delta\Delta S$ for the parent vs. variant unfolding transitions is independent of temperature over this range. Given that assumption, the sum of the differential stability values for the mesophile (Fig. 4A) and hyperthermophile (Fig. 4B) proteins yields the difference between the sum of the thermodynamic stabilities for the pair of complementary hybrids vs. the corresponding sum for the parental rubredoxins (Fig. 4C). There is only a small difference in the sum of the thermodynamic stabilities of the pair of residue 24 variants vs. that of the parental rubredoxins, although this difference is larger than the estimated uncertainty. The corresponding differences in stability for the interchanges of only residue 33 and for residues 24 and 33 together are yet smaller. Fitting to a two-state model yields the thermodynamic parameters of the thermal transitions given in Table 1.

Within the experimental uncertainty, the increase in thermodynamic stability upon the simultaneous substitution of V24I and I33L into the *Cp* wild type protein is equal to the decrease in thermodynamic stability for the complementary double-residue substitution into *Pf* A2K rubredoxin. Given the previously estimated 5.8 kcal/mol difference in free energy between the parental proteins, the thermodynamic additivity demonstrated for the double mutant indicates that the 1.2 kcal/mol change that occurs upon the simultaneous exchange of residues 24 and 33 accounts for 21% of the difference in stability between the *Cp* and *Pf* A2K rubredoxins. The interchange of residue 33 alone accounts for ~14% of that difference in stability between the parental proteins.

With the exception of the covalent structural changes due to conversion of Ile to Val at positions 24 and Leu to Ile at position 33, the crystallographic study reported essentially no differences for the triple mutant vs. the wild type structure [34] in the region surrounding these two aliphatic residues. Hence, the triple mutant rubredoxin appears to maximally preserve the parental-like interactions within this region of the protein. Although the corresponding structure for the complementary triple mutant of *Cp* rubredoxin has not been determined, the additivity in thermodynamic stability observed in the present study strongly suggest that a similar preservation of parental-like local interactions occur for this rubredoxin variant as well.

3.3. Interchange of the nonconserved aromatic residue in the hydrophobic core

The residues shown in Fig. 1 form much of the hydrophobic core of the protein. Also included in the core are the aromatic rings of Tyr 11, Phe 49, and residue 4 (Tyr in *Cp* rubredoxin and Trp in *Pf* rubredoxin). Kinetic stability measurements monitoring the loss of the metal binding interactions during prolonged incubation at elevated temperatures revealed no difference in apparent stability at neutral pH between the wild type and the W4Y, I24V, L33I triple mutant of *Pf* rubredoxin [17] (using *Cp* rubredoxin numbering), although at pH 2 the triple mutant irreversibly denatures more rapidly [16].

When Tyr 4 is substituted into the I24V, L33I variant of *Pf* A2K rubredoxin, the thermal transition temperature decreases (★, Fig. 3B). Similarly, substitution of tryptophan at residue 4

Table 1
Rubredoxin thermal transition parameters

	Tm[a]	ΔH_{T_m}[b]
Cp wt	107.0(0.3)	62
V24I	109.5(0.3)	59
I33L	111.8(0.2)	64
V24I,I33L	115.2(0.4)	65
Y4W,V24I,I33L	113.7(0.5)	63
Pf A2K	138.8(0.4)	81
I24V	136.1(0.4)	74
L33I	134.3(0.4)	73
I24V,L33I	132.7(0.5)	62
W4Y,I24V,L33I	128.8(0.4)	66

[a]Uncertainty estimated from independent fits of the individual resonances to the Gibbs–Helmholtz equation assuming a common ΔH_{T_m}.
[b]Enthalpy of unfolding (kcal/mol).

in the V24I, I33L variant of *Cp* rubredoxin also yields a decrease in T_m (★, Fig. 3A). Fig. 4b shows the thermodynamic stability of the W4Y, I24V, L33I triple mutant of *Pf* A2K rubredoxin referenced against the I24V, L33I double mutant. The data for the complementary Y4W, V24I, I33L triple mutant of *Cp* rubredoxin are illustrated in Fig. 4a. In both cases, the triple mutant is less stable than are the related double mutants, indicating that the additivity in thermodynamic stability observed for these double mutants no longer holds true when residue 4 is exchanged. The interchange of residue 4 yields a net 0.78 kcal/mol deviation from additivity in thermodynamic stability.

A number of changes in the X-ray structures were observed surrounding the exchanged aromatic ring. Most notably, the indole H^N of Trp 4 in the wild type *Pf* rubredoxin forms a direct hydrogen bond to the buried sidechain carboxylate of Glu 15 and a water-mediated hydrogen bond to the sidechain of Glu 31. Although the sidechain of the substituted tyrosine in the triple mutant structure is precisely superimposed upon the position of the indole, the lateral displacement of the phenolic hydroxyl results in a direct hydrogen bond to the Glu 31 sidechain carboxylate, while a water-mediated hydrogen bond to the Glu 15 carboxylate is formed. A similar exchange of hydrogen bond interactions likely applies to the parental and aromatic substituted *Pf* A2K rubredoxins studied herein. On the other hand, the N-terminal ammonium group in the wild type *Pf* rubredoxin also forms a salt-bridge with the Glu 15 carboxylate sidechain. When the N-terminal methionine is not removed by post-translational processing, the Ala 2 amide hydrogen of *Pf* rubredoxin then forms a presumably weaker hydrogen bond to the Glu 15 carboxylate [24], as likely occurs in the *Pf* A2K rubredoxin variant as well.

The 0.52 kcal/mol decrease in thermodynamic stability that arises from the substitution of tyrosine for tryptophan in the structural context of the I24V, L33I variant of *Pf* A2K rubredoxin indicates that this aromatic residue accounts for at most 9% of the differential stability between the parental *Cp* and *Pf* A2K proteins. However, the differing interactions of the N-terminus of wild type *Pf* rubredoxin may give rise to a larger differential stability contribution for this residue.

A relatively small differential stability effect of residue 4 was anticipated from our previous analysis of a complementary pair of rubredoxin hybrids in which the multi-turn segment of the protein sequence (residues 14–33) was interchanged [25]. Although the complementary pair of hybrids interchanging the 20 residue multi-turn segment between *Cp* and *Pf* A2K rubredoxin do not conform to the non-interacting cluster criterion used to predict the metal binding site cluster and the residue 24 and 33 cluster, they exhibit an 83% additivity in their thermodynamic stabilities relative to the parental proteins [25]. The putative hybridization interface was generated by removing the multi-turn residues from the parental rubredoxin crystal structure [35]. One face of the aromatic ring of residue 4 was found to present the only interface atoms that are not structurally conserved between the parental rubredoxins. The near additivity in thermodynamic stability of these two multi-turn segment-swapped rubredoxins indicate that interchanging a substantial fraction of the interactions for the sidechain of residue 4 occurs at a modest cost in free energy.

4. Conclusions

To date, there are few cases in which moderately large differential stabilities between evolutionarily related proteins can be quantitatively interpreted in terms of the incremental contributions of specific nonconserved residues. Combined with our earlier reported stability measurements on the metal binding site cluster [13], the additivity in the thermodynamic stability exhibited by the two residue cluster for positions 24 and 33 demonstrate that the nonconserved residues of *Cp* and *Pf* A2K rubredoxins can be cleanly divided into three sets that account for 39%, 21% and 40% of the differential thermodynamic stability for the parental proteins. Given the algorithmic basis for the cluster selection, it will be of interest to see how applicable this analysis approach will be to other homologous pairs of moderately divergent proteins.

Exploiting the property of additivity in thermodynamic stability, the metal binding site-swapped hybrids of rubredoxin have also been shown to exhibit a property of additivity of conformational dynamics as monitored by hydrogen exchange kinetics [36]. This approach appears to offer a promising avenue to characterizing the propagation of conformational dynamics through the structure of a protein. Analogous studies on the residues 24 and 33 cluster will provide further insight into the generality of this approach.

Acknowledgments

We acknowledge the use of the Wadsworth Center NMR facility and Molecular Genetics Core as well as the technical assistance of Lynn McNaughton and Jianzhong Tang. This work was supported in part by NIH Grant GM 64736 (G.H.).

References

[1] D. Perl, U. Mueller, U. Heinemann, F.X. Schmid, Two exposed amino acid residues confer thermostability on a cold shock protein, Nat. Struct. Biol. 7 (2000) 380–383.
[2] D. Perl, F.X. Schmid, Electrostatic stabilization of a thermophilic cold shock protein, J. Mol. Biol. 313 (2001) 343–357.
[3] J. Hasegawa, H. Shimahara, M. Mizutani, S. Uchiyama, H. Arai, M. Ishii, Y. Kobayashi, S.J. Ferguson, Y. Sambongi, Y. Igarashi, Stabilization of *Pseudomonas aeruginosa* cytochrome *c*551 by systematic amino acid substitutions based on the structure of thermophilic *Hydrogenobacter thermophilus* cytochrome *c*552, J. Biol. Chem. 274 (1999) 37533–37537.
[4] K. Oikawa, S. Nakamura, T. Sonoyama, A. Ohshima, Y. Kobayashi, S.J. Takayama, Y. Yamamoto, S. Uchiyama, J. Hasegawa, Y. Sambongi, Five amino acid residues responsible for the high stability of *Hydrogenobacter thermophilus* cytochrome *c*552, J. Biol. Chem. 280 (2005) 5527–5532.
[5] A. Matouschek, A.R. Fersht, Protein engineering in analysis of protein folding pathways and stability, Methods Enzymol. 202 (1991) 82–112.
[6] A. Horovitz, Double-mutant cycles: a powerful tool for analyzing protein structure and function, Fold. Des. 1 (1996) R121–R126.
[7] G. Hernández, D.M. LeMaster, Hybrid native partitioning of the interactions among nonconserved residues in chimeric proteins, Proteins: Struct., Funct., Bioinf. 60 (2005) 723–731.
[8] M.W. Day, B.T. Hsu, L. Joshua-Tor, J.B. Park, Z.H. Zhou, M.W.W. Adams, D.C. Rees, X-ray crystal structures of the oxidized and reduced forms of the rubredoxin from the marine hyperthermophilic archaebacterium *Pyrococcus furiosus*, Prot. Sci. 1 (1992) 1494–1507.
[9] P.R. Blake, J.B. Park, Z.H. Zhou, D.R. Hare, M.W.W. Adams, M.F. Summers, Solution-state structure by NMR of zinc-substituted rubredoxin

from the marine hyperthermophilic archaebacterium *Pyrococcus furiosus*, Prot. Sci. 1 (1992) 1508–1521.
[10] B.S. McCrary, S.P. Edmondson, J.W. Shriver, Hyperthermophile protein folding thermodynamics: differential scanning calorimetry and chemical denaturation of Sac7d, J. Mol. Biol. 264 (1996) 784–805.
[11] X. Zhang, W. Meining, M. Fischer, A. Bacher, R. Ladenstein, X-ray structure analysis and crystallographic refinement of lumazine synthase from the hyperthermophile *Aquifex aeolicus* at 1.6 Å Resolution: determinants of thermostability revealed from structural comparisons, J. Mol. Biol. 306 (2001) 1099–1114.
[12] D.M. LeMaster, J. Tang, G. Hernández, Absence of kinetic thermal stabilization in a hyperthermophile rubredoxin indicated by 40 microsecond folding in the presence of irreversible denaturation, Proteins: Struct., Funct., Bioinf. 57 (2004) 118–127.
[13] D.M. LeMaster, G. Hernández, Additivity in both thermodynamic stability and thermal transition temperature for rubredoxin chimeras via hybrid native partitioning, Structure 13 (2005) 1153–1163.
[14] J. Vondrášek, L. Bendová, V. Klusák, P. Hobza, Unexpectedly strong energy stabilization inside the hydrophobic core of small protein rubredoxin mediated by aromatic residues: correlated ab initio quantum chemical calculations, J. Am. Chem. Soc. 127 (2005) 2615–2619.
[15] K.E. Riley, J.K.M. Merz, Role of solvation in the energy stabilization inside the hydrophobic core of the protein rubredoxin, J. Phys. Chem., B 110 (2006) 15650–15653.
[16] T. Chatake, K. Kurihara, I. Tanaka, I. Tsyba, R. Bau, F.E. Jenney, M.W.W. Adams, N. Niimura, A neutron crystallographic analysis of a rubredoxin mutant at 1.6 Å resolution, Acta Crystallogr., D Biol. Crystallogr. 60 (2004) 1364–1373.
[17] E.R. Zartler, F.E. Jeeney, M. Terrell, M.K. Eidsness, M.W.W. Adams, J.H. Prestegard, Structural basis for thermostability in aporubredoxins from *Pyrococcus furiosus* and *Clostridium pasteurianum*, Biochemistry 40 (2001) 7279–7290.
[18] J. Tang, G. Hernández, D.M. LeMaster, Increased peptide deformylase activity for the N-formylmethionine processing of proteins overexpressed in *Escherichia coli*: application to homogeneous rubredoxin production, Protein Expr. Purif. 36 (2004) 100–105.
[19] M.K. Eidsness, K.A. Richie, A.E. Burden, D.M. Kurtz, R.A. Scott, Dissecting contributions to the thermostability of *Pyrococcus furiosus* rubredoxin: beta-sheet chimeras, Biochemistry 36 (1997) 10406–10413.
[20] G. Hernández, D.M. LeMaster, Reduced temperature dependence of collective conformational opening in a hyperthermophile rubredoxin, Biochemistry 40 (2001) 14384–14391.
[21] M.R. Arnold, W. Kremer, H.D. Lüdemann, H.R. Kalbitzer, 1H-NMR parameters of common amino acid residues measured in aqueous solutions of the linear tetrapeptides Gly-Gly-X-Ala at pressures between 0.1 and 200 MPa, Biophys. Chemist. 96 (2002) 129–140.
[22] J.K. Myers, C.N. Pace, J.M. Scholtz, Denaturant m values and heat-capacity changes: relation to changes in accessible surface areas of protein folding, Prot. Sci. 4 (1995) 2138–2148.
[23] Z. Dauter, K.S. Wilson, L.C. Sieker, J.M. Moulis, J. Meyer, Zinc- and iron-rubredoxin from *Clostridium pasteurianum* at atomic resolution: a high-precision model of a ZnS4 coordination unit in a protein, Proc. Natl. Acad. Sci. U. S. A. 93 (1996) 8836–8840.
[24] R. Bau, D.C. Rees, D.M. Kurtz, R.A. Scott, H.S. Huang, M.W.W. Adams, M.K. Eidsness, Crystal-structure of rubredoxin from *Pyrococcus furiosus* at 0.95 Angstrom resolution, and the structures of N-terminal methionine and formylmethionine variants of *Pf* Rd. Contributions of N-terminal interactions to thermostability, J. Biol. Inorg. Chem. 3 (1998) 484–493.
[25] D.M. LeMaster, J. Tang, D.I. Paredes, G. Hernández, Contribution of the multi-turn segment in the reversible thermal stability of hyperthermophile rubredoxin: NMR thermal chemical exchange analysis of sequence hybrids, Biophys. Chemist. 116 (2005) 57–65.
[26] G.S. Huang, T.G. Oas, Submillisecond folding of monomeric λ repressor, Proc. Natl. Acad. Sci. U. S. A. 92 (1995) 6878–6882.
[27] R.E. Burton, G.S. Huang, M.A. Daughterty, P.W. Fullbright, T.G. Oas, Microsecond protein folding through a compact transition state, J. Mol. Biol. 263 (1996) 311–322.
[28] B. Kuhlman, J.A. Boice, R. Fairman, D.P. Raleigh, Structure and stability of the N-terminal domain of the ribosomal protein L9: evidence for rapid two-state folding, Biochemistry 37 (1998) 1025–1032.
[29] S. Spector, D.P. Raleigh, Submillisecond folding of the peripheral subunit-binding domain, J. Mol. Biol. 293 (1999) 763–768.
[30] J.K. Myers, T.G. Oas, Preorganized secondary structure as an important determinant of fast protein folding, Nat. Struct. Biol. 8 (2001) 552–558.
[31] U. Mayor, N.R. Guydosh, C.M. Johnson, J.G. Grossmann, S. Sato, G.S. Jas, S.M.V. Freund, D.O.V. Alonso, V. Daggett, A.R. Fersht, The complete folding pathway of a protein from nanoseconds to microseconds, Nature 421 (2003) 863–867.
[32] K.A. Bava, M.M. Gromiha, H. Uedaira, K. Kitajima, A. Sarai, ProTherm, Version 4.0: thermodynamic database for proteins and mutants, Nucleic Acids Res. 32 (2004) D120–D121.
[33] A.T. Clark, B.S. McCrary, S.P. Edmondson, J.W. Shriver, Thermodynamics of core hydrophobicity and packing in the hyperthermophile protein Sac7d and Sso7d, Biochemistry 43 (2004) 2840–2853.
[34] K. Kurihara, I. Tanaka, T. Chatake, M.W.W. Adams, J.F.E. Jenney, N. Moiseeva, R. Bau, N. Niimura, Neutron crystallographic study on rubredoxin from *Pyrococcus furiosus* by BIX-3, a single-crystal diffractometer for biomacromolecules, Proc. Natl. Acad. Sci. U. S. A. 101 (2004) 11215–11220.
[35] K.D. Watenpaugh, L.C. Sieker, L.H. Jensen, Crystallographic refinement of rubredoxin at 1.2 Å resolution, J. Mol. Biol. 138 (1980) 615–633.
[36] D.M. LeMaster, G. Hernández, Additivity of differential conformational dynamics in hyperthermophile/mesophile rubredoxin chimeras as monitored by hydrogen exchange, Chem. Bio. Chem. 7 (2006) (web edition).